Preliminary Numerical Assessment of the Towing Resistance of a Floating Offshore Wind Platform in Calm Water

Hugo Ferreiro-Gómez
CEHINAV, ETSIN
Universidad Politécnica de Madrid
Madrid, Spain
h.ferreiro@alumnos.upm.es

Jordi Mas-Soler
Naval Arch. & Ocean Eng. Department
Esc. Politécnica, Universidade de São Paulo (USP)
University of São Paulo, Brazil
ORCID:0000-0001-6528-9018

***Abstract*—This paper offers a comprehensive examination of towing resistance simulations in calm water for the CENTEC-TLP model, providing a comparative analysis with experimental data. Using the open-source software OpenFOAM®, a verification and validation process for the mesh is provided to ensure the accuracy of results. The simulations systematically address the intricate dynamics linked to the free trim and sinkage of the platform, exploring two distinct towing configurations over a range of towing velocities. The study includes in-depth comparative analyses, integrating the scrutiny of wake fields and wave heights, strategically aligning these observations with experimental images for an assessment of the simulation outcomes.**

***Index Terms*—OpenFOAM, Numerical Towing Resistance, TLP platform, calm water.**

I. Introduction

Offshore wind energy is recognized as a significant source of clean energy in a scenario with increasing demand for renewable sources. In recent years the development of floating substructures has gained attention, since it allows the exploration of the wind potential in regions with large water depths, where the fixed foundation are not technically feasible or economical. In this context, harnessing of offshore wind resources involves the installation of numerous wind turbines to form a wind farm. During the installation process, the towing operation of the platform, carried out by two or more tugboats depending on the platform's size and hull geometry, must be repeated numerous times. As an example, we can mention the project registered by Petrobras [3], with a total installed capacity of 3.2MW, set to be installed 42km off the coast of Rio de Janeiro, Brazil, comprising a total of 178 wind turbines. This project illustrates the scale of the towing operation and its potential impact on project costs, given the total number of platforms to be installed and the distance from the coast.

The examination of specific details related to the towing operations of floating wind turbines, particularly concerning platform resistance, lacks comprehensive research. Previous studies (see [5] and [1]) focused on assessing the towing resistance of a TLP-type floating wind turbine. More recently, [6] contributed a numerical study that explores an innovative platform concept. Additionally, in [9], the authors conducted an experimental campaign to characterize towing resistance in both calm water and waves for the CENTEC-TLP concept [11]. However, there remains a notable gap in the extensive investigation of the specifics surrounding towing operations and platform resistance for floating wind turbines.

Within this framework, the aim of this work is to conduct a preliminary numerical assessment, utilizing the OpenFOAM® software, of the towing resistance in calm water for the CENTEC-TLP concept [11]. The towing resistance of the concept in calm water and in waves has been experimentally studied previously in [9], indicating that the tugboat necessary for the towing operation would be of the 20 tonnes range.This works also includes the validation of the established methodology by comparing the numerical estimations with experimental data from a towing tank, as reported in [9].

The following two sections outline the methodology and provide an insight into the main features of the platform. Section IV describes the test matrix, and Section V discusses and analyzes the results. Finally, the paper concludes by summarizing the main conclusions and proposing directions for future research.

II. Methodology

The software OpenFOAM® was used to estimate the resistance of the platform. A general outline is given in this section, mentioning the governing equations behind the solver and the discretization schemes utilized.

OpenFOAM® employs the volume of fluid (VOF) method to determine the properties of the cells in each *timeStep*. In case of multiphase problems, the Equation 1 expresses the fraction of each fluid that exists in each cell, reproducing in the analysed case the free surface elevation.

$$\frac{\partial \alpha}{\partial t} + \nabla(\alpha \mathbf{u}) = 0 \tag{1}$$

where α stands for volume fraction (*alpha.water*) and $\mathbf{u}$ is the flow velocity.

The governing equations to solve the problem are the Navier-Stokes equations, which are provided in vector form by Equation 2, for incompressible two-phase flow momentum, and by Equation 3 for continuity. These equations are included in the multiphase solver applied, *InterFoam*. A detailed explanation of the solver is provided in [7].

$$\frac{\partial \mathbf{u}}{\partial t} + (\mathbf{u} \cdot \nabla)\mathbf{u} - \nu \nabla^2 \mathbf{u} = -\frac{1}{\rho}\nabla p + \mathbf{g}. \quad (2)$$

$$\nabla \cdot \mathbf{u} = 0 \quad (3)$$

To discretize the governing equations, the finite volume method (FVM) is used in *fvSchemes*. Linear interpolation , namely (*Gauss linear*, *Gauss linearUpwind*), is utilized for the divergence terms, with the exception of $div(phi, alpha)$ where a second order scheme (*Gauss vanLeer*) is applied. To enhance the convergence in each *timeStep*, the PIMPLE algorithm is employed, following the recommendations provided by*Wolf Dynamics* in [2].

For the turbulence model, the *kOmega-SST* RAS is adopted to accurately capture the free surface elevation and provide a robust representation of the boundary layer, as detailed in [8].

In an effort to reduce computational time, the initial five seconds were run with the constrained platform, followed by a ramp for applying damping coefficients until the tenth second.

III. Case study

The following subsections provide a concise overview of the key features pertaining to the platform hull, simulation mesh, and computational resources.

A. Platform model

The platform geometry was based on the CENTEC-TLP [11], already tested in the tank of the CEHINAV [9] at a model scale of 1:60. The platform dimensions replicated those of the model, and the specific parameters are detailed in Table I.

TABLE I
Parameters of the TLP model introduced in OpenFOAM.

Parameters	Symbol	Value	Units
Length	L	0.817	[m]
Draft	T	0.064	[m]
Mass	m	8.100	[kg]
Z position of gravity center	KG	0.458	[m]
Pitch inertia	I_{55}	0.545	[kg·m^2]

Geometry dimensional data was used to set the distance from the object to the boundaries, and at the same time, to define the dimensions of the refinement boxes. The remaining parameters were introduced in `dynamicMmeshDict` to replicate the behaviour of the platform in heave and pitch motions.

The geometry of the TLP introduced in OpenFOAM®, see Figure 1, was trimmed at a height of 0.175m, equivalent to 10.5m in full scale, from the baseline. This geometry modification aimed to reduce the number of cells generated to form the wall of the body.

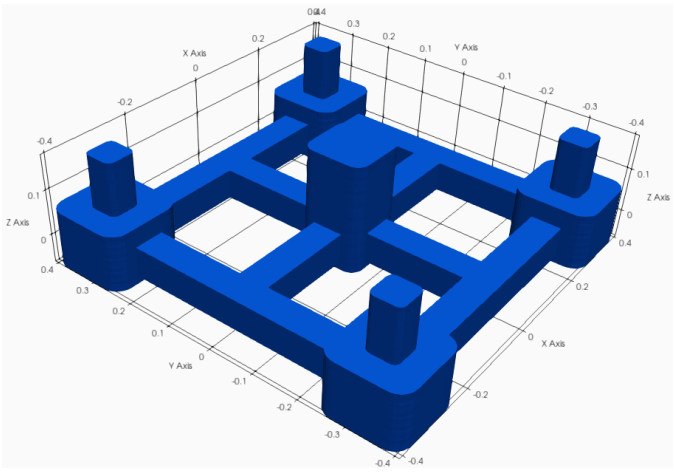

Fig. 1. Geometry of the CENTEC-TLP scaled model (1:60).

B. Simulation Mesh

In his study, different meshes were generated to assess and verify their quality. The verification and validation were made for the diagonal configuration, see Figure 4, at a full scale equivalent towing speed of 5kn. Figure 2 shows the relative error between experimental data and numerical results as a function of the number of cells. The mesh had a hexahedral

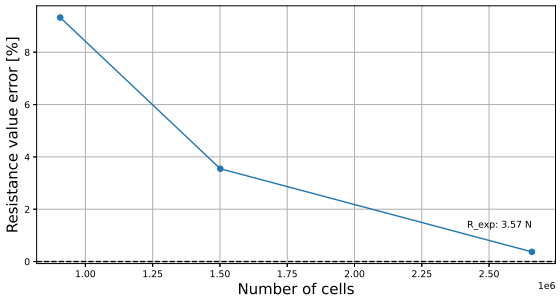

Fig. 2. Difference between experimental and numerical values in function of the number of cells.

structure with different levels of refinement, with half of the size of the previous cell at each level down. Three levels of refinement were made around the platform plus an extra one surrounding the walls of the body to reproduce the effect of boundary layer, see Figure 3. In the free surface, two levels of refinement were made in order to capture the influence of the multiphase region without increasing the number of cells. The mesh setup was the same for both configurations assessed, changing the orientation of the platform to match the towing configuration as described in Section IV.

Following the mesh validation, the research was carried out with a cell count of 2.65M of cells. This decision was based on the considerations of the error magnitude, particularly noting that at lower velocities, errors tend to be more prominent due to the less well-defined nature of the boundary layer.

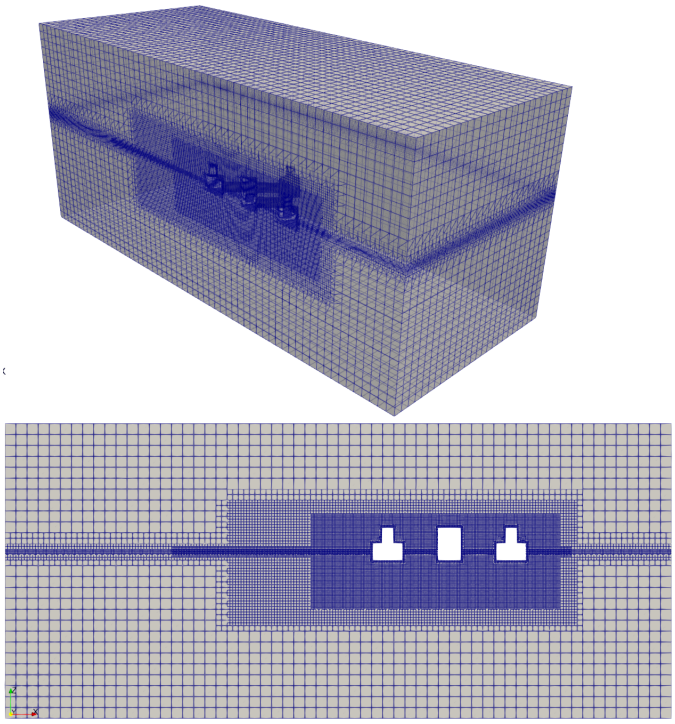

Fig. 3. Mesh built for analyzing towing resistance—top view depicted in 3D and bottom view in 2D for one of the two towing configurations under evaluation.

C. Computational Resource

Simulations were performed in a cluster, but always in one node for each simulation. The computers had the following characteristics: Intel®Xeon®Gold processors, with 20 cores, 64GB RAM, and 1TB SSD disk for data writing.

The processing time varied for each simulation, despite that, the average time recorded for the simulations was 9.5 hours using 16 processors. The simulation duration was established at 30 seconds, employing a constant time step of 0.01s. These decisions were guided by the convergence observed in initial test cases and considerations of the *Courant Number*, aiming for a balanced trade-off between stability and accuracy in the simulations.

IV. Test matrix and numerical set-up

A. Test matrix

The experimental program included multiple speeds in two towing configurations, see Figure 4. In the simulations just the orientation towards the flow was considered. The towing point was dismissed, as in [9] directional instabilities were not observed while towing the platform in the experimental campaign and no relevant differences in the resistance were observed due to this fact.

The Table II compiles the entire set of simulations, encompassing speeds up to 6 knots (full scale) for the two towing configurations. The mesh generation process remained consistent for both platform tow configurations, as discussed in Section III. However, it is noteworthy that a disparity in the number of cells between the frontal and diagonal cases is observable. This discrepancy arises due to the hexahedral meshing methodology[4] employed in OpenFOAM®.

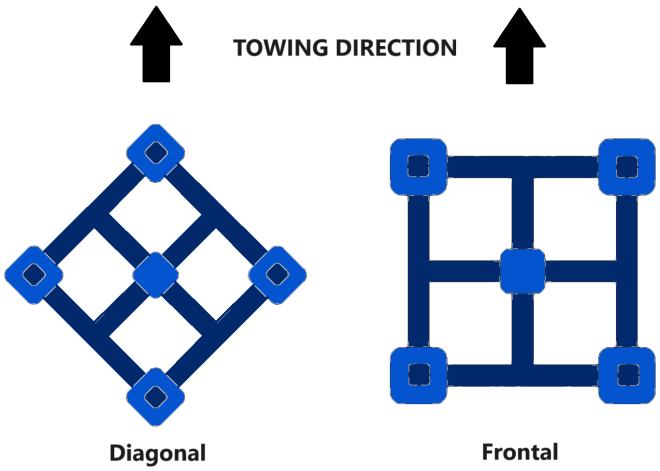

Fig. 4. Towing configurations simulated.

TABLE II
Simulation Set.

Set id.	Speed[kn]	Tow Config.	N. Cells[M]
1	1	Diagonal	2.659
2	2	Diagonal	2.659
3	3	Diagonal	2.659
4	4	Diagonal	2.659
5	5	Diagonal	2.659
6	6	Diagonal	2.659
7	1	Frontal	2.214
8	2	Frontal	2.214
9	3	Frontal	2.214

B. Numerical Set-up

The simulations were run in parallel, decomposed in 16 partitions by the *hierarchical* method. The parameters used to run the simulation and the boundary conditions are shown in Table III. The remaining boundaries, not shown in Table III, were subject to a symmetry condition.

Initial reference values of k and *omega* were: 5.952e-06 and 0.5952, respectively. The calculation of these parameters was made using the tool in [10].

V. Results

The outcomes for each case and the disparities from the corresponding experimental data are provided in Table IV.

Overall, a satisfactory agreement is observed between the numerical and experimental estimations of towing resistance. However, significant deviations, with an error up to 37.7%, from the experimental data become apparent at towing speeds of 1 and 2 kn, in the diagonal configuration. Additionally, a significant discrepancy is also noted at the 2 kn towing speed for the frontal configuration. These variations can be attributed

TABLE III
TRANSPORT PROPERTIES & BOUNDARY CONDITIONS.

Parameters	**Symbol**	**Value**	**Unit**
Water density	ρ_{water}	998.8	[kg/m^3]
Air density	ρ_{air}	1.0	[kg/m^3]
Water kinematic viscosity	ν_{water}	1.09e-06	[m^2/s]
Air kinematic viscosity	ν_{air}	1.48e-05	[m^2/s]

Boundary conditions

	Inlet	**Outlet**	**Atmosphere**	**Platform**
alpha.water	FV	VHFR	IO	ZG
k	FV	IO	IO	kqRWF
nut	FV	ZG	ZG	nutkRWF
omega	FV	IO	IO	omegaWF
p_rgh	FFP	ZG	TP	FFP
U	FV	OPMV	PIOV	MWV

TABLE IV
COMPARISON OF TOWING RESISTANCE ESTIMATES BETWEEN NUMERICAL SIMULATIONS AND EXPERIMENTAL DATA (FULL SCALE).

Set id.	Exp.Data[KN]	OF Results[KN]	Error[%]
1	2.933	4.038	37.7
2	10.835	8.962	17.3
3	25.014	24.891	0.5
4	51.073	47.120	7.7
5	79.270	78.976	0.4
6	113.926	111.765	1.9
7	2.566	2.795	8.9
8	9.051	7.631	15.7
9	19.669	20.453	4.0

to the less well-defined nature of the boundary layer and the limit of fully turbulent flow, as discussed in Section III.

The results are additionally presented graphically, offering a visual representation of the resistance curves for both configurations in contrast to the experimental data. These curves are depicted in Figure 5 and Figure 6, complementing the data previously provided in Table IV.

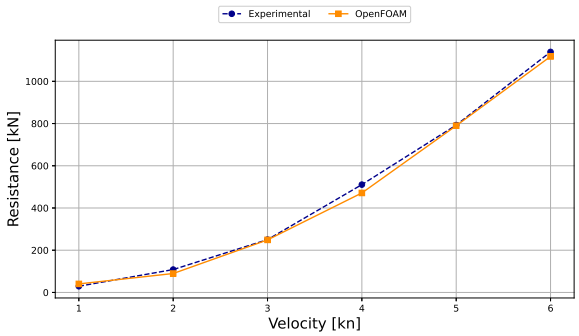

Fig. 5. Resistance Curve Comparison for diagonal towing Configuration.

The comparison of resistance numerical results, for the two towing configurations, albeit restricted to three towing speeds,

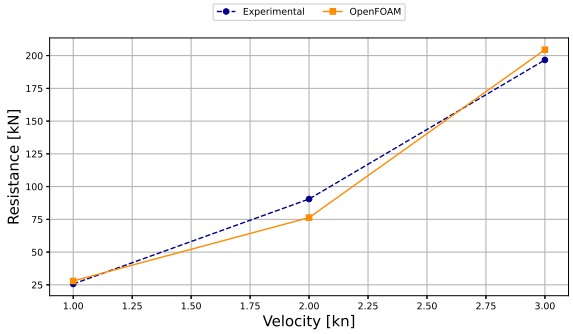

Fig. 6. Resistance Curve Comparison for frontal towing configuration

suggests a potentially faster increase in towing resistance for the diagonal configuration, with additional 4.66KN (numerical) and 5.35kN (experimental) to the towing resistance for the frontal configuration at an equivalent full scale speed of 3kn. This observed behavior may be attributed to the platform's dynamics and the specific characteristics of the hull geometry. Nevertheless, a comprehensive investigation into this matter is deferred to future work.

In addition to the resistance results, Figure 7 and Figure 8, provide images capturing wave generation and the wake at an equivalent full-scale towing speed of 5kn.

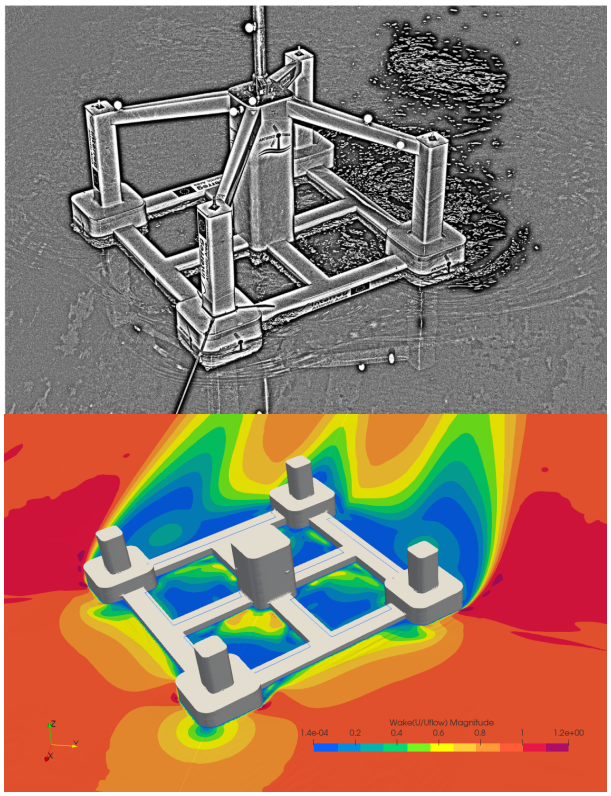

Fig. 7. Wake comparison between image in experiments [9] and OpenFOAM results at 5kn. - Top view experimental wake and bottom view, CFD wake

To facilitate a comparative analysis regarding the impact of

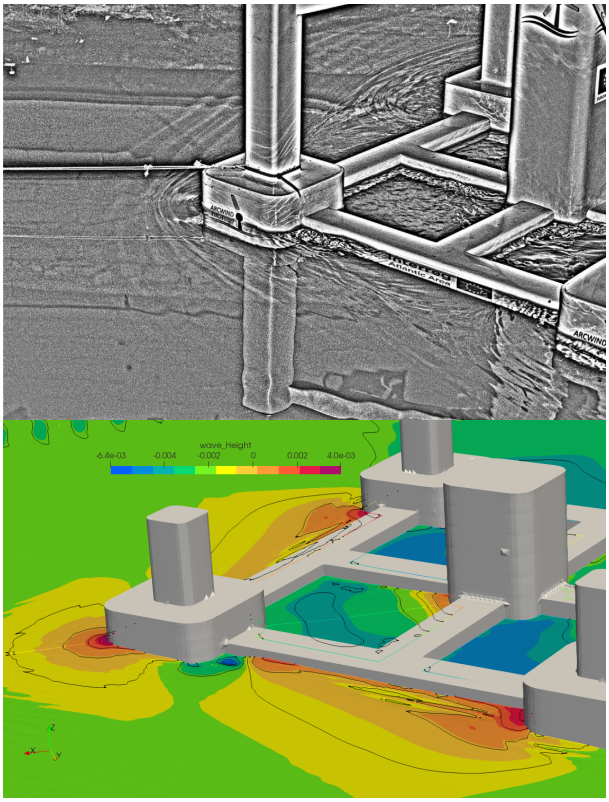

Fig. 8. Wave height and wake distortion comparison between image in experiments [9] and OpenFOAM results at 5kn. - Top view experimental wake and bottom view, CFD wave height.

omitting the towing cable in the simulation on downstream wake formation, Figure 7 and Figure 8 also include experimental images as presented in [9].

In Figure 7, the wake pattern of the platform appears comparable between the simulated and experimental cases at an equivalent full-speed of 5 kn. In both instances, the flow accelerates at the farthest inboard pontoon, indicated by the dark red color in the bottom view and a curve of bubbles in the top view. Conversely, Figure 8 reveals a depression in the frontal pontoon observed after the corner, depicted in blue in the CFD simulation.

VI. Conclusions

The comparison between empirical and numerical resistance curves reveals a strong correlation in the results. However, a more in-depth analysis of the frontal towing configuration at higher speeds remains a subject for future investigation.

The error analysis, particularly for the diagonal configuration, attests to the strong correlation between the experimental and numerical results for higher velocities, while larger errors are anticipated at lower speeds. This aligns with the expected trend of improved agreement as towing velocity increases, attributed to a less defined boundary layer at lower speeds.

The observed accelerated increase in towing resistance for the diagonal configuration, in contrast to the frontal configuration, as highlighted in the resistance comparison, is hypothesized to stem from the interplay of platform dynamics and hull geometry. A comprehensive exploration of this phenomenon has been left for future research.

The visual examination of wake patterns reveals comparable behavior between simulated and experimental cases, suggesting similarities in the flow patterns around the hull of the platform.

Future work will additionally focus on developing a methodology for towing resistance in head waves and conducting a comprehensive analysis of the TLP model's results. This research will maintain continuity with the set of waves and velocities outlined in [9].

Acknowledgment

The authors acknowledge the computational resources received from the "Tanque de Provas Numérico. Universidade de São Paulo" (TPN) and the "Centro de Supercomputación y Visualización de Madrid" (CeSViMA). The authors would also like to thank Javier Calderón Sánchez and Alexandre Nicolaos Simos for the help in developing the simulations and issues related with the hydrodynamic approach.

References

[1] Juan Amate, Gustavo D Sánchez, and Gonzalo González. Development of a semi-submersible barge for the installation of a tlp floating substructure. tlpwind® case study. In Journal of Physics: Conference Series, volume 749, page 012016. IOP Publishing, 2016.

[2] Wolf Dynamics. Tips and tricks in OpenFOAM®. http://www.wolfdynamics.com/wiki/tipsandtricks.pdf, 2014. Accessed: 3-12-2023.

[3] EPNBR. Petrobras registra primeiro projeto de eólica offshore flutuante do brasil. https://epbr.com.br/petrobras-anuncia-projeto-de-eolica-offshore-flutuante-no-rj/, 2022. Accessed: 3-12-2023.

[4] OpenFOAM ESI. Mesh generation with the snappyhexmesh utility. https://www.openfoam.com/documentation/user-guide/4-mesh-generation-and-conversion/4.4-mesh-generation-with-the-snappyhexmesh-utility. Accessed: 3-12-2023.

[5] Thomas Hyland, Frank Adam, Frank Dahlias, and Jochen Großmann. Towing tests with the gicon®-tlp for wind turbines. In ISOPE International Ocean and Polar Engineering Conference, pages ISOPE–I. ISOPE, 2014.

[6] E. Henriques J. Cardoso, M. Vieira and L. Reis. Computational analysis of the transportation phase of an innovative foundation for offshore wind turbine. Ships and Offshore Structures, 16(7):725–734, 2021.

[7] Hrvoje Jasak. Openfoam: Open source cfd in research and industry. International Journal of Naval Architecture and Ocean Engineering, 1(2):89–94, 2009.

[8] Bjarke Larsen and David Fuhrman. On the overproduction of turbulence beneath surface waves in reynolds-averaged navier–stokes models. Journal of Fluid Mechanics, 853:419–460, 10 2018.

[9] Jordi Mas-Soler, Emre Uzunoglu, Gabriele Bulian, C. Guedes Soares, and Antonio Souto-Iglesias. An experimental study on transporting a free-float capable tension leg platform for a 10 mw wind turbine in waves. Renewable Energy, 179:2158–2173, 2021.

[10] CFD Online. Turbulence properties, conversions boundary estimations. https://www.cfd-online.com/Tools/turbulence.php. Accessed: 3-12-2023.

[11] Emre Uzunoglu and C. Guedes Soares. Hydrodynamic design of a free-float capable tension leg platform for a 10 mw wind turbine. Ocean Engineering, 197:106888, 2020.